

Conformational Adaptation of Human Cytochrome P450 2B6 and Rabbit Cytochrome P450 2B4 Revealed upon Binding Multiple Amlodipine Molecules

Manish B. Shah,^{*,†} P. Ross Wilderman,[†] Jaime Pascual,[‡] Qinghai Zhang,[§] C. David Stout,[§] and James R. Halpert[†]

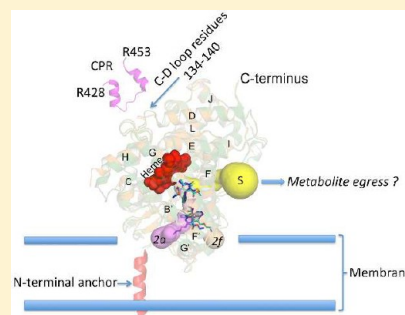
[†]Skaggs School of Pharmacy and Pharmaceutical Sciences, University of California, San Diego, La Jolla, California 92093, United States

[‡]Department of Molecular and Experimental Medicine, The Scripps Research Institute, La Jolla, California 92037, United States

[§]Department of Molecular Biology, The Scripps Research Institute, La Jolla, California 92037, United States

S Supporting Information

ABSTRACT: Structures of human cytochrome P450 2B6 and rabbit cytochrome P450 2B4 in complex with two molecules of the calcium channel blocker amlodipine have been determined by X-ray crystallography. The presence of two drug molecules suggests clear substrate access channels in each P450. According to a previously established nomenclature, amlodipine molecules were trapped in access pathway 2*f* in P450 2B6 and in pathway 2*a* or 2*f* in P450 2B4. These pathways overlap for part of the length and then diverge as they extend toward the protein surface. A previously described solvent channel was also found in each enzyme. The results indicate that key residues located on the surface and at the entrance of the substrate access channels in each of these P450s may play a crucial role in guiding substrate entry. In addition, the region of P450 2B6 and 2B4 involving helices B', F, F', and G' and part of helix G is substantially more open in the amlodipine complexes than in the corresponding 4-(4-chlorophenyl)imidazole complexes. The increased active site volume observed results from the major retraction of helices F, F', and B' and the β 4 sheet region located close to the binding cavity to accommodate amlodipine. These structures demonstrate novel insight into distinct conformational states not observed with previous P450 2B structures and provide clear evidence of the substrate access channels in two drug-metabolizing P450s. In addition, the structures exhibit the versatility that can be exploited via in silico studies with other P450 2B6 ligands as large as raloxifene and itraconazole.



Cytochrome P450 (P450) enzymes make up a superfamily of monooxygenases involved in the metabolism of a vast array of xenobiotics.¹ In addition to their critical role in drug clearance, these heme-containing enzymes are involved in the biosynthesis of steroids and prostaglandins and can also oxidize a wide variety of endogenous fatty acids.² X-ray crystal structures and biochemical analysis of cytochromes P450 have led to a wealth of information regarding their substrate specificity and conformational flexibility.

The anchoring of microsomal P450s into the membrane occurs primarily via an N-terminal transmembrane segment, although the enzymes retain membrane binding properties even upon removal of this domain.³ Our laboratory has used N-terminally truncated and engineered constructs of P450 2B enzymes with internal mutations to achieve the increased solubility, purity, and stability required for biophysical and structural studies.⁴ Various techniques such as site-directed mutagenesis, isothermal titration calorimetry, and deuterium-exchange mass spectrometry have been employed previously to characterize the members of the 2B subfamily, primarily rat P450 2B1 and rabbit P450 2B4.^{5–7} Additionally, as a result of its superior solubility compared with those of other 2B

enzymes, P450 2B4 has been an excellent model for X-ray crystallography. To date, a total of 12 structures of P450 2B4 have been determined. There are six structures that represent closed conformations of the enzyme in complex with small imidazole inhibitors, the antiplatelet drugs ticlopidine and clopidogrel, and the covalently bound mechanism-based inactivator *tert*-butylphenylacetylene.^{8,9} There are also two distinct ligand-free structures, one open and one closed,^{7,10} as well as one expanded¹¹ and three intermediate^{9,12} conformations with various inhibitors.

Of the 57 human P450 enzymes identified, P450 2B6 contributes extensively to the metabolism of pharmaceuticals that include bupropion, efavirenz, propofol, selegiline, and artemisinin.¹³ Moreover, human P450 2B6 is known for its polymorphic nature, with Q172H and K262R representing the most common amino acid substitutions. Years of research efforts spent on expression, purification, and crystallization have recently led to the determination of the structure of a human

Received: July 3, 2012

Revised: August 8, 2012

Published: August 21, 2012



P450 2B6 genetic variant in complex with the nonpharmaceutical ligands 4-(4-chlorophenyl)imidazole (4CPI), 4-benzylpyridine (4BP), and 4-(4-nitrobenzyl)pyridine (4NBP), yielding details about the rearrangement of active site residues to accommodate small inhibitors.^{14,15} However, information about the conformational behavior of P450 2B4 and 2B6 in the presence of bulkier ligands and/or clinical drugs has been lacking. Interestingly, recent structural analysis of bacterial P450_{cam} revealed distinct conformational states of the protein in the presence or absence of ligand and demonstrated the role of certain secondary structural elements in the conformational changes.¹⁶

The substrate access or exit channels that connect the protein surface to the deeply buried active site have been defined previously in several P450s using X-ray crystallography and molecular dynamics (MD) studies. The structure of P450 2C8 revealed channels on either side of helix B' extending to the solvent from the buried active site,¹⁷ while the P450 2E1 structure described the location of the channel as being between the B–B' loop, the β_1 sheet system, and beneath helices F' and G'.¹⁸ However, in the vitamin D 25-hydroxylase P450 2R1 structure, vitamin D3 enters the active site via a channel between helices G and I, the B' helix, and the B–C loop,¹⁹ whereas helices B' and F and the β_1 sheet region form such an access channel in the cholesterol hydroxylase P450 46A1 structure.²⁰ In addition, the recent structural analysis of Cyp51 revealed substrate access channels near the F–G loop, helix A', and the β_4 loop.²¹ It is noteworthy that MD simulations of P450 2C9 and P450 3A4 demonstrated opening and closing of several putative substrate access and exit channels.^{22,23} Our understanding of substrate access–egress channels was advanced substantially by the recent determination of structures of dual ligand complexes of P450 2A1, P450 101D2, P450 21A2, and P450 2A13.^{24–27} The second ligand molecule was located at a distal site in a channel extending to the protein surface near the B–B' loop, β_1 sheet, and F–G loop in P450 2A1; near helices B' and F/G and the F–G loop in P450 101D2; between the β_1 – β_2 and β_3 – β_4 loops and helix F' in P450 21A2; and close to the β_4 sheet system, above the K'–L loop in P450 2A13. Accordingly, the existing evidence suggests that the diversity of substrate access channels results from intrinsic differences in the P450s as well as structural differences among the substrates.

An intriguing feature of P450 2B enzymes is the ability to bind ligands of widely diverse size and shape. This may reflect not only the flexibility of the active site but also the dynamic nature of the access channel(s). To elucidate how substrates can gain access to the buried active site in human P450 2B6 and rabbit P450 2B4 and to determine the conformational flexibility in the presence of larger drugs, X-ray crystallography studies were initiated using P450 2B4^a in complex with amlodipine (Figure 1 of the Supporting Information). Amlodipine is a calcium channel blocker drug used in the treatment of hypertension and coronary artery disease and has been previously shown to inhibit human P450 2B6 with high affinity.^{28,29} Subsequently, P450 2B6^b was crystallized in the presence of amlodipine. The resulting structures reveal substrate access channels with two molecules of drug bound to both the rabbit and human P450 2B enzymes and demonstrate the movement of the structural elements important for substrate access and binding.

MATERIALS AND METHODS

Materials. Amlodipine besylate was obtained from Sigma-Aldrich (St. Louis, MO). CHAPS was from Calbiochem (EMD Chemicals, San Diego, CA). CYMAL-5 (5-cyclohexyl-1-pentyl- β -D-maltoside) was acquired from Anatrache (Maumee, OH). Nickel-nitrilotriacetic (Ni^{2+} -NTA) acid affinity resin was from Thermo Scientific (Rockford, IL). Macroprep CM cation-exchange resin was received from Bio-Rad Laboratories (Hercules, CA). Amicon ultrafiltration devices were from Millipore (Billerica, MA). The pGro7 plasmid was from Takara Bio (Shiba, Japan). *Escherichia coli* JM109 and TOPP3 cells were from Stratagene (La Jolla, CA). Crystal Screen HR2-110 and the Wizard II crystallization screen were from Hampton Research (Aliso Viejo, CA) and Emerald Biosciences (Seattle, WA), respectively. 3(R)-Hydroxy-7(R),12(R)-bis(ethoxy)-cholane (234-chol) is a custom-made facial amphiphile.³⁰ All protein figures were created using PyMOL.³¹ BKchem version 0.13.0 (2009, <http://bkchem.zirael.org/index.html>) was used for drawing the chemical structure of amlodipine.

Expression and Purification of Rabbit P450 2B4 and Human P450 2B6. Cytochrome P450 2B4 was heterologously expressed as described previously.⁷ Briefly, an overnight Luria-Bertani broth culture of *E. coli* TOPP3 cells containing the cDNA for 2B4dH(H226Y) in the pKK2B4 plasmid was used to inoculate Terrific broth in the presence of tetracycline and ampicillin. Terrific broth cultures were grown until A_{600} reached approximately 0.7 at 37 °C. Isopropyl β -D-1-thiogalactopyranoside and δ -aminolevulinic acid were added to final concentrations of 0.5 and 1 mM, respectively, and protein expression was induced for 72 h at 30 °C. Cells were harvested by centrifugation at 4000g and resuspended in 10% of the original culture volume in buffer containing 20 mM potassium phosphate (pH 7.4 at 4 °C), 20% (v/v) glycerol, 10 mM 2-mercaptoethanol (BME), and 0.5 mM phenylmethanesulfonyl fluoride (PMSF). The cell suspension was treated with lysozyme (0.3 mg/mL) for 2 h at 4 °C and centrifuged at 8000g. The resulting spheroplasts were then resuspended in 5% of the original culture volume in buffer containing 500 mM potassium phosphate (pH 7.4 at 4 °C), 20% (v/v) glycerol, 10 mM BME, and 0.5 mM PMSF and sonicated on ice. The detergent CHAPS was added to a final concentration of 0.8% (w/v), and the sample was stirred for 90 min at 4 °C before being subjected to ultracentrifugation for 45 min at 245000g in a Beckman Coulter Optima L-80 XP Ultracentrifuge using a Ti 50.2 rotor. The concentration of P450 in the supernatant was measured using the reduced CO difference spectra.³²

Histidine-tagged P450 2B4 was purified using nickel affinity chromatography in the presence of CHAPS. The protein-bound Ni^{2+} -NTA column was washed using buffer containing 100 mM potassium phosphate (pH 7.4 at 4 °C), 100 mM NaCl, 20% (v/v) glycerol, 10 mM BME, 0.5 mM PMSF, 0.5% CHAPS, and 5 mM histidine. The protein was eluted using the buffer described above containing 50 mM histidine. The P450-containing fractions were pooled and quantitated as described above prior to being diluted in buffer with 5 mM potassium phosphate (pH 7.4 at 4 °C), 20% (v/v) glycerol, 1 mM ethylenediaminetetraacetic acid (EDTA), 0.2 mM dithiothreitol (DTT), 0.5 mM PMSF, and 0.5% (w/v) CHAPS. The protein was then loaded onto a Macroprep CM column that was washed using the buffer containing 50 mM potassium phosphate (pH 7.4 at 4 °C), 20 mM NaCl, 20% (v/v) glycerol, 1 mM EDTA, and 0.2 mM DTT and eluted with the buffer

described above containing 500 mM NaCl. Protein fractions containing protein of the highest quality as measured by the A_{417}/A_{280} ratios were pooled, and the P450 concentration was measured using the reduced CO difference spectra.³²

Heterologous expression of P450 2B6 was conducted in *E. coli* JM109 cells containing the pKK2B6dH (Y226H/K262R) plasmid. In addition, GroEL/ES chaperones (pGro7 plasmid) were co-expressed with the pKK2B6 plasmid as described previously.^{15,33} The purification protocol was exactly the same as that described above for P450 2B4 except that 150 μ M amlodipine from a stock solution in DMSO was included in all the buffers used throughout the purification of P450 2B6. Crystals of the P450 2B6–amlodipine complex were not obtained without such inclusion of amlodipine during the purification procedure.

Crystallization and Data Collection. Two milliliters of each pooled sample of P450 2B4 and P450 2B6 from the ion-exchange column was diluted to 18 μ M in 50 mM potassium phosphate (pH 7.4 at 4 °C), 500 mM NaCl, 500 mM sucrose, 1 mM EDTA, and 0.2 mM DTT. Amlodipine was added to a final concentration of 180 μ M. P450 2B4 and P450 2B6 were concentrated to 550 and 280 μ M, respectively, by centrifugation using 50 kDa molecular mass cutoff Amicon Ultrafiltration devices. The protein aliquots were again diluted to 18 μ M with the buffer described above containing amlodipine at a concentration of 180 μ M. This process was repeated twice before each aliquot was concentrated to final concentrations of 550 and 280 μ M, respectively. The concentrated protein samples were supplemented with 4.8 mM CYMAL-5 and 0.077% (w/v) 234-cho¹⁵ before crystallization. Crystal screening for P450 2B4 and P450 2B6 was performed by the sitting drop vapor diffusion method. Crystals of P450 2B4 were obtained from the Wizard II screen (Emerald Biosciences) at 18 °C after the protein had been incubated for 7 days at a 1:1 ratio with the precipitant containing 1 M K/Na tartrate, 0.1 M Tris (pH 7), and 0.2 M Li₂SO₄.

Crystals of P450 2B6 grew over a period of 1 month after the protein had been incubated at 18 °C in a 1:1 ratio with the precipitant containing 0.2 M sodium acetate trihydrate, 0.1 M Tris-HCl (pH 8.5), and 30% (w/v) PEG4000 using Crystal Screen HR2-110 from Hampton Research. Crystals of P450 2B4 and P450 2B6 were transferred to mother liquor containing 20% (v/v) sucrose as a cryoprotectant before being flash-frozen in liquid nitrogen. Crystallographic data were collected on each P450 crystal remotely at Stanford Synchrotron Radiation Lightsource (SSRL) beamline 11-1³⁴ (2B4) and 7-1³⁴ (2B6) using 1° oscillations over 240 frames and 20 s exposures using a Marmosaic 325 CCD detector for the P450 2B4 crystal and a Quantum 315 CCD detector for the P450 2B6 crystal at 100 K. Crystals of P450 2B4 diffracted to 2.25 Å, while crystals of human P450 2B6 diffracted to 2.8 Å. Data were integrated using iMOSFLM³⁵ and scaled via SCALA in CCP4i.³⁶

Structure Determination and Refinement. To determine the structure of P450 2B4, coordinates of the closed ligand-free P450 2B4 structure (PDB entry 3MVR) were used as a search model in the molecular replacement program Phaser³⁷ in CCP4i. The space group was determined to be $P3_121$, and Matthews coefficient determination suggested the presence of one molecule in the asymmetric unit with 67.8% solvent content. The output model from Phaser was submitted to rigid body and restrained refinement in REFMAC,³⁸ and COOT³⁹ was used to further build the model using $F_o - F_c$ and

$2F_o - F_c$ electron density maps contoured at 3σ and 1σ , respectively. The library description for amlodipine was created using the PRODRG server.⁴⁰ Iterative model building and refinement was continued until the R factor and R_{free} stopped improving. The overall geometry of the structure analyzed by MOLPROBITY⁴¹ ranked in the 98th percentile among structures of comparable resolution, with no Ramachandran outliers or bad bond lengths or angles. The final model of the crystal structure contains protein residues 28–492, with the terminal histidine residue being a part of the larger C-terminal His tag. There were 206 water molecules found in the model, and a single CYMAL-5 detergent molecule was observed in the hydrophobic pocket near residues Phe202 and Phe296. In addition, during refinement, two alternate conformations of the amlodipine chlorophenyl ring were observed in the molecule ligated to heme. Residue 136, located within the C–D loop region, which was previously shown to interact with cytochrome P450 reductase,⁴² was disordered in the final model. This was probably due to high mobility and is consistent with several other P450 2B4 structures. Moreover, density for residue 48 was missing, as was part of density for the side chains of R49 and R73, which thus were not modeled. Coordinates and structure factors were deposited as PDB entry 3TMZ. The refinement statistics for the structure described above are summarized in Table 1.

The structure of P450 2B6 was determined using the automated molecular replacement pipeline Balbes.⁴³ The space group was found to be $P2_12_12_1$, containing 52.3% solvent, assuming two monomers per asymmetric unit. A solution was determined using the P450 2B6–4CPI structure (PDB entry 3IBD) from the PDB as the search model. The output model was subjected to a rigid body refinement and a restrained refinement in REFMAC using the tight noncrystallographic symmetry options. The water molecules were added manually, and the iterative process of model building and refinement yielded the final R factor and R_{free} values of 0.24 and 0.29, respectively. MOLPROBITY⁴¹ analysis, which scored the structure at the 91st percentile among structures of comparable resolution with no Ramachandran outliers, is presented in Table 1, along with overall geometry and final refinement statistics of the structure. The final model of P450 2B6 consisted of residues 28–492 in chain A and chain B as observed with P450 2B4, and 78 water molecules. Density for residues 28, 280, and 281 in chain B was poorly defined so they could not be modeled. The atomic coordinates and structure factors were deposited as PDB entry 3UA5.

Determination of Substrate Access Channels in P450 2B4 and P450 2B6 and Active Site Cavity Volume Calculations. The substrate access channels in P450 2B4 and P450 2B6 were analyzed using CAVER.⁴⁴ The water, CYMAL-5, and amlodipine molecules were deleted from the coordinates of P450 2B4 and P450 2B6 chain A, and the region above the active site heme iron was chosen as the starting point of access channel calculation using a 4 Å probe in CAVER. PyMOL³¹ was used for visualizing the substrate access channels. Active site cavity volumes of the P450 2B–amlodipine complexes were calculated using Voidoo,⁴⁵ and probe-occupied volumes were determined with a probe radius of 1.40 Å. Because of the connection between the active site and the substrate access channel $2f$ leading to the protein exterior (vide infra), water molecules were added at the location of the second molecule of amlodipine to limit the active site to the region surrounding the first amlodipine.

Table 1. Data Collection and Refinement Statistics^a

	2B4	2B6
ligand	amlodipine	
crystal space group	<i>P</i> 3 ₁ 21	<i>P</i> 2 ₁ 2 ₁ 2 ₁
crystal unit cell parameters		
<i>a</i> (Å)	92.9	58.0
<i>b</i> (Å)	92.9	78.3
<i>c</i> (Å)	152.7	247.3
$\alpha = \beta$ (deg)	90	90
γ (deg)	120	90
no. of molecules per asymmetric unit	1	2
Data Collection ^a		
beamline	SSRL 11-1	SSRL 7-1
wavelength (Å)	0.98	0.98
resolution range (Å)	38.93–2.25	82.45–2.80
completeness (%)	96.4 (65.0)	90.4 (82.5)
redundancy	6.2 (3.3)	4.3 (3.2)
<i>R</i> _{merge} (%)	4.3 (49.8)	13.1 (60.3)
<i>I</i> / σ	13.6 (1.5)	4.7 (1.3)
no. of unique reflections	36346	25912
Refinement		
<i>R</i> factor (%)	19.1	24.2
<i>R</i> _{free} (%)	25.1	29.4
rmsd		
bond lengths (Å)	0.023	0.012
bond angles (deg)	2.085	1.430
no. of atoms [average <i>B</i> value (Å ²) in parentheses]		
protein	3694 (48.3)	7379 (50.8)
heme	43 (33.4)	86 (38.2)
proximal amlodipine	28 (47.06)	28 (48.9)
distal amlodipine	28 (80.2)	28 (67)
water	203 (51.2)	78 (36.34)
detergent	34 (86.3)	0
Ramachandran plot (%)		
preferred	96.7	94.7
allowed	3.3	5.3

Values for the highest-resolution shell are in parentheses.

Ligand Docking. Docking of amlodipine, raloxifene, and itraconazole into the amlodipine-bound complexes of 2B4 (PDB entry 3TMZ) and 2B6 (PDB entry 3UAS) was accomplished by using AutoDock Vina version 1.1.1.⁴⁶ Residues not modeled into the experimental electron density were added using COOT, and amlodipine and CYMAL-5 molecules were removed from the file. Experiments were performed with a rigid receptor molecule, and Gasteiger charges were utilized for the small molecule. Heme charges were modified using a separate script to provide previously reported values.⁴⁷ The docking experiment included 20 events with a 70 Å × 70 Å × 70 Å box centered on the heme iron.

Enzyme Inhibition Studies. Rates of O-dealkylation of 7-ethoxy-4-(trifluoromethyl)coumarin (7-EFC) and 7-methoxy-4-(trifluoromethyl)coumarin (7-MFC) to the metabolite 7-hydroxy-4-(trifluoromethyl)coumarin for P450 2B4 and P450 2B6, respectively, were measured using a fluorometric assay. A reconstituted enzyme system contained P450 2B4 or P450 2B6, rat cytochrome P450 reductase (CPR), and rat cytochrome *b*₅⁴⁸ at a molar ratio of 1:4:2. The reactions were performed in a 100 μL volume containing 50 mM HEPES (pH 7.4), 15 mM MgCl₂, 10 pmol of P450, 40 pmol of CPR, 20 pmol of cytochrome *b*₅, 50 μM 7-EFC for P450 2B4 or 7-MFC for P450

2B6, and 0–1 mM amlodipine. Reactions were initiated by adding NADPH after preincubation for 5 min at 37 °C. Trichloroacetic acid [20% (v/v)] was added to quench the reaction after incubation for 5 min. In addition, a single reaction was terminated without the addition of substrate in a control experiment. An F-2000 fluorescence spectrophotometer (Hitachi, Tokyo, Japan) with a λ_{ex} at 410 nm and a λ_{em} at 500 nm was used to measure the fluorescence, and the IC₅₀ values were determined using the Michaelis–Menten equation with the scientific package Igor Pro 6.1 (Wavemetrics, Inc., Lake Oswego, OR). IC₅₀ values of 2 and 1.6 μM were determined for inhibition by amlodipine of P450 2B4 and P450 2B6, respectively. These values were similar to the previously reported values using wild-type P450 2B6.²⁹

RESULTS

Structural Analysis of Complexes of P450 2B4 and P450 2B6 with Amlodipine. Crystal structures of P450 2B4 and P450 2B6 were determined in the presence of amlodipine at 2.25 and 2.8 Å resolution, respectively. The structures described here displayed the global P450 fold and similar overall conformation to each other. Unbiased electron density for the drug amlodipine (Figure 1A,B and Figure 2 of the Supporting Information) was clearly observed bound to heme in P450 2B4 and P450 2B6 via the amine nitrogen atom. In addition, unbiased electron density for another molecule of amlodipine near the active site was located close to the first molecule in both enzymes. The second molecule of amlodipine in P450 2B6 was found in an orientation different from that in P450 2B4. Attempts to model the second amlodipine molecule observed in P450 2B4 in the orientation similar to that of the second amlodipine in P450 2B6 resulted in the *B* values becoming worse. The two P450 2B6 molecules present in the asymmetric unit are identical to each other with a root-mean-square deviation (rmsd) of 0.1 Å for the C α atoms between chains A and B. The complete structures of P450 2B4 and P450 2B6 are shown in panels C and D of Figure 1, respectively.

Panels A and B of Figure 2 show the residues located within a 5 Å radius of either amlodipine molecule in P450 2B4 or P450 2B6. The residues found within that radius around the heme-bound amlodipine molecule in the active site are located mainly on the B–C loop and helices F and I in each of these proteins. The orientation of amlodipine and the majority of the active site residues are identical in both enzymes (Table 1A of the Supporting Information), except for residues T300 and C475 in P450 2B4 and R98 and V104 in P450 2B6, which move out of the 5 Å radius in the other structure. C475 in P450 2B6 and V104 in P450 2B4 have been shown previously to interact with ligands in the active site in other 2B structures.^{49,50} The F206 and F297 side chains, which were shown recently to rearrange to accommodate various ligands within the active site of human P450 2B6,¹⁵ were found in the same orientations observed in the respective P450 2B4 and 2B6 4CPI complexes.

The second molecule of amlodipine was sandwiched between helices F, F', A', and A in both P450 2B4 and P450 2B6, suggesting a secondary binding site for the ligand. Additionally, as listed in Table 1B of the Supporting Information, 15 residues in P450 2B4 (Figure 2A) and 17 residues in P450 2B6 (Figure 2B) are within a 5 Å radius of this amlodipine. In P450 2B4, the chlorophenyl moiety and the ethyl ester of this secondary amlodipine face helices A and A', respectively, while the amine nitrogen orients toward the

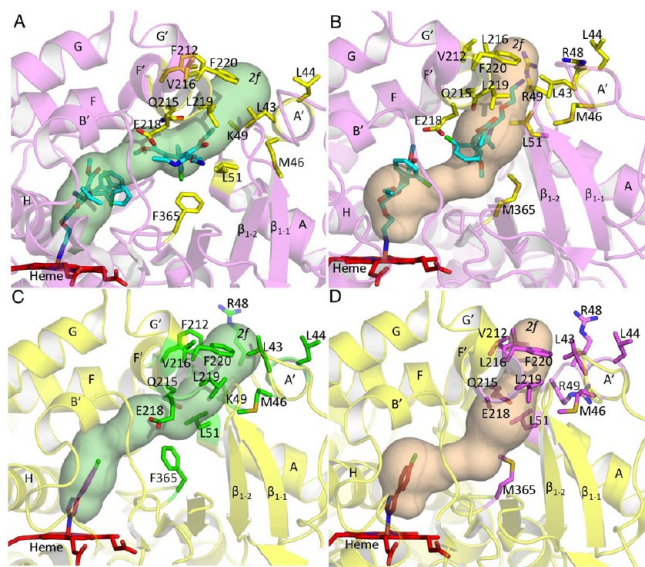


Figure 3. Substrate access channel 2*f* shown in P450 2B4 and P450 2B6 as computed by CAVER, and the residues located at the channel entrance. Heme is colored red, and amlodipine and 4CPI molecules are colored cyan and orange, respectively. Tunnels are labeled according to the previously defined nomenclature.⁵³ In addition, residue 365 located further in the substrate access channel is also shown to represent the marked movement of the side chain. (A) Channel 2*f* observed in the P450 2B4–amlodipine complex (magenta) and the residues (yellow sticks) located at the entrance of the channel. (B) Substrate access channel 2*f* found to open in the human P450 2B6 amlodipine complex and the residues (yellow sticks) located at the channel entrance. (C and D) Corresponding residues in the P450 2B4–4CPI (green sticks) and P450 2B6–4CPI (magenta sticks) complexes, respectively, that protrude into channel 2*f* of the P450 2B4–amlodipine (yellow) and P450 2B6–amlodipine (magenta) complexes.

L51, Q215, and E218, which protrude into the channel in the 4CPI complexes, move out in the amlodipine complexes. Interestingly, F365 in P450 2B4 flips by more than 60° compared with the 4CPI complex to make space for the chlorophenyl ring of the second amlodipine molecule. This movement also contributes to opening of channel 2*f* in P450 2B4. Such a marked movement of residue M365 is not observed in P450 2B6, mainly because of an alternate conformation of amlodipine. However, the sulfur side chain of methionine does move out slightly to accommodate the methyl ester group of amlodipine.

Further analysis revealed a second substrate access channel in P450 2B4 between helices B' and G' near the β_1 sheet system (Figure 4A). Comparison of the corresponding residues lining the channel entrance with P450 2C9 indicates that this channel

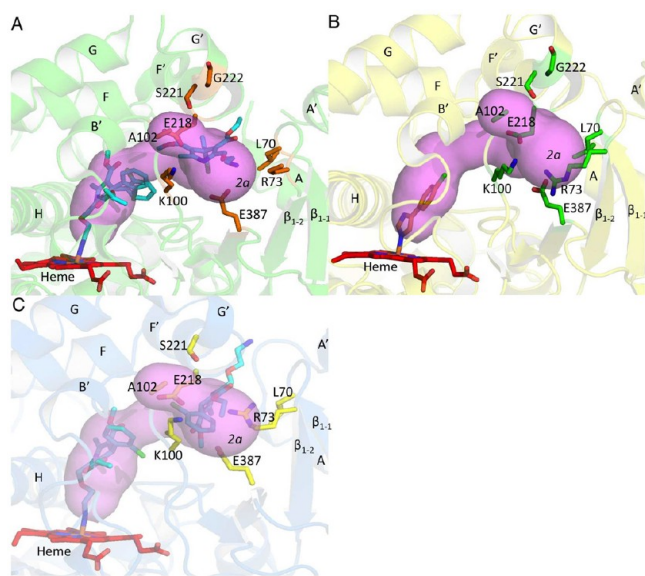


Figure 4. Substrate access channel 2*a* as computed by CAVER. (A) Access channel 2*a* observed in the P450 2B4–amlodipine complex and residues located at the entrance near the protein surface shown as orange sticks. The primary amine of amlodipine (cyan sticks) is seen to extend near the entrance of channel 2*a*. (B) Corresponding residues in the P450 2B4–4CPI complex that need to move shown as green sticks near channel 2*a* of the amlodipine complex. (C) Access channel 2*a* not observed in P450 2B6 mainly as a result of R73 (yellow sticks), which projects into the channel entrance. The primary amine tail of amlodipine (cyan sticks) is now seen to extend at the entrance of channel 2*f*.

closely resembles channel 2*a* according to the nomenclature (Table 2). Additionally, as seen from comparison of Figures 3A and 4A, channels 2*a* and 2*f* start at the same location and then diverge as they extend toward the protein surface. In the P450 2B4–4CPI complex, channel 2*a* is blocked by E218 on helix F' and R73 on the β_{1-2} sheet, which protrude into the channel (Figure 4B). The movement of helix F' as a result of amlodipine binding displaces E218 in both P450 2B complexes, which contributes to branching of channels 2*f* and 2*a* in P450 2B4 and P450 2B6. However, channel 2*a* is blocked in the P450 2B6–amlodipine structure (Figure 4C) because of the orientation of R73. In P450 2B4, the density for the guanidino group of R73 is missing, but on the basis of the side chain carbons that are observed, the group must point away from this channel toward the solvent. This side chain orientation opens branched out channel 2*a* in P450 2B4. The presumed high mobility of R73 likely allows it to avoid any clash with the primary amine of amlodipine in P450 2B4. Residues lining the entrance of this tunnel are R73, K100, A102, and E387 on the β_1 sheet system and S221 on helix G'.

Table 2. Residues and Secondary Structural Elements Located at the Entrance Channels in P450 2B4 and P450 2B6 Along with the Corresponding Residues in P450 2C9 Proposed Previously

channel	residues lining the access channels			secondary structure
	P450 2B4	P450 2B6	P450 2C9	
solvent	S207, E301, R308, V477	S207, E301, R308, V477	C206, E300, R307, F476	helices E, F, and I, β_4 sheet
2 <i>f</i>	P38, L43, M46, R48, F212, V216, L219, G222	P38, L43, M46, R48, V212, L216, L219, G222	P37, I42, I45, I47, I215, N218, P211, P221	helices F', G', A', and A
2 <i>a</i>	L70, R73, A102, S221, G222	L70, R73, A102, S221, G222	K69, K72, P101, S220, P221	helices F' and G', β_1 sheets

The solvent channel, which has been described previously in several MD simulation and structural studies,^{24,51,54–57} was located between helices F and I and the β_4 loop region near helix E. A recent study of P450 2C9⁵¹ predicted that the solvent channel is used for metabolite egress because of the polar residues lining the channel. However, this channel may also be involved in substrate entry. The residues lining the entrance of this channel in P450 2B4 and P450 2B6 are listed in Table 2 along with the corresponding residues previously suggested in P450 2C9. In the P450 2B4–4CPI complex, the side chain of residue F203 protrudes into the solvent channel, while in the amlodipine complex, F203 flips $\sim 90^\circ$ outward to open this channel, thus creating a large access pathway for the substrate or metabolite to possibly enter or egress (Figure 3 of the Supporting Information). In P450 2B6, residue 203 is a tyrosine and is observed to move $\sim 30^\circ$ compared with the 4CPI complex (Figure 4 of the Supporting Information). Again, this creates significantly more room for larger ligands. Additionally, residue E474 in P450 2B6 flips away from the channel by $\sim 180^\circ$, allowing C475 to be closer to the access path than in the 4CPI complex. Such displacement of E474 in P450 2B4 by $\sim 90^\circ$ is also observed compared with the respective P450 2B4–4CPI complex, creating an even larger space for the solvent channel. The roles of E474 and C475 have been investigated recently in P450 2B4 and P450 2B6, respectively, using site-directed mutagenesis. The P450 2B4 E474 mutants exhibited a significant change in binding affinity with several ligands, while the P450 2B6 C475S mutants showed altered mechanism-based inactivation by 2-oxo clopidogrel.^{50,58}

Conformational and Active Site Adaptations of P450 2B4 and P450 2B6 upon Amlodipine Binding.

An overlay of the structure of the P450 2B4–amlodipine complex onto the open ligand-free structure of the protein¹⁰ and the closed conformation of the 4CPI complex⁴⁹ is shown in Figure 5A. The closed 4CPI-bound conformation of P450 2B4 is essentially identical to the closed ligand-free structure (rmsd of 0.49 Å) as well as the complexes with the drugs ticlopidine or clopidogrel (rmsd's of 0.37 and 0.32 Å, respectively). Relative to these closed P450 2B4 structures, the P450 2B4–amlodipine complex exhibits a substantial displacement of helices F, F', G', and G, which coordinate as a unit, and of helices A', A, and B'. Additionally, the β_{1-1} and β_{1-2} sheets were also displaced considerably. The average rmsd between the structure of the amlodipine complex and the closed 2B4 structures was 0.66 Å, with the largest differences resulting from the movement of the secondary structural elements discussed above. A comparison with the open ligand-free 2B4 structure reveals changes in the orientations of helices I and C and the G–H and H–I loops, in addition to similar differences seen in the closed conformation structures. In the active site, eight additional residues (R98, F206, I209, S210, P368, and three glycines at positions 299, 366, and 478) compared with the 4CPI complex of P450 2B4 circumscribe the bulkier amlodipine molecule. Interestingly, each of these additional contact residues has been shown to contact ligands in the active site in at least one of the previously determined ligand-bound structures of P450 2B4.⁵⁹

When compared to the 4CPI complex, the binding of the much larger amlodipine results in significant alteration of the size and topology of the active site (Figure 5B,C), yielding an active site cavity (605 Å³) that is much larger than that previously observed in P450 2B4 structures such as the 4CPI complex (253 Å³).⁸ This difference results from the location

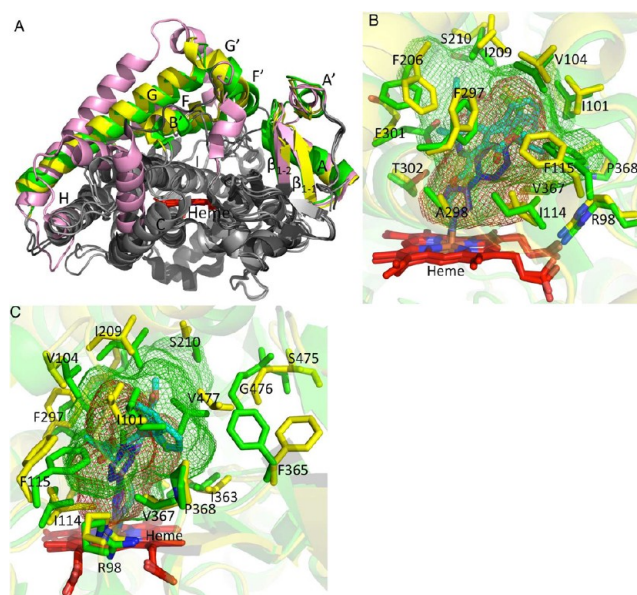


Figure 5. Overlay of P450 2B4 structures. (A) Superimposed structures of the P450 2B4–amlodipine complex (yellow), P450 2B4 open ligand-free (PDB entry 1PO5) (pink), and 4CPI (PDB entry 1SUO)-bound (green) structures with secondary structural elements that are displaced colored as described above. Ligand molecules were removed for the sake of clarity. (B and C) Overlay of residues in sticks lining the active sites of the P450 2B4–amlodipine (yellow) and P450 2B4–4CPI (green) complexes (these panels are orthogonal views of the same figure). The cavity volume of the P450 2B4–amlodipine complex (green mesh) is increased significantly upon movement of active site residues. The cavity volume of the P450 2B4–4CPI complex is shown as red mesh. Amlodipine and 4-CPI molecules are colored cyan and blue, respectively.

and orientation of the residues that line the heme-binding pocket region. α displacement by ~ 2 Å in the amlodipine relative to the 4CPI complex was observed for S475, G476, and V477 located near the β_4 sheet region in P450 2B4. In addition, the backbone of residues I101 and V104 and residues I209 and S210 on helices B' and F, respectively, were retracted considerably by ~ 1.5 Å compared with those in the 4CPI complex. Moreover, the cluster of phenylalanine residues F115, F206, F297, and F365 exhibited marked side chain adjustments to accommodate amlodipine, and E301 and F365 rotate out in the amlodipine complex, further contributing to the enlarged binding cavity.

While structural studies have revealed a range of P450 2B4 conformations, human P450 2B6 has been crystallized only in the presence of the small inhibitors 4CPI, 4BP, and 4NBP, resulting in similar closed protein structures. The conformational changes observed in the P450 2B6–amlodipine complex when compared with the previously determined closed conformation structures described above were more pronounced (average rmsd of 0.88 Å) than in P450 2B4. Binding of amlodipine to P450 2B6 is accompanied by conformational shifts of the G–H loop and helices A', A, B', F, F', G', G, and H (Figure 6A). Moreover, there were marked differences between the amlodipine and 4CPI complexes of P450 2B6 near the C-terminal coil (the β_{3-3} sheet, helix L', and the β_{4-1} , β_{4-2} , and β_{3-2} region), as compared with the corresponding P450 2B4 structures (Figure 5 of the Supporting Information). The β_{4-1} and β_{4-2} sheets observed in the 4CPI complexes of the respective P450s are now seen as a continuous loop extending

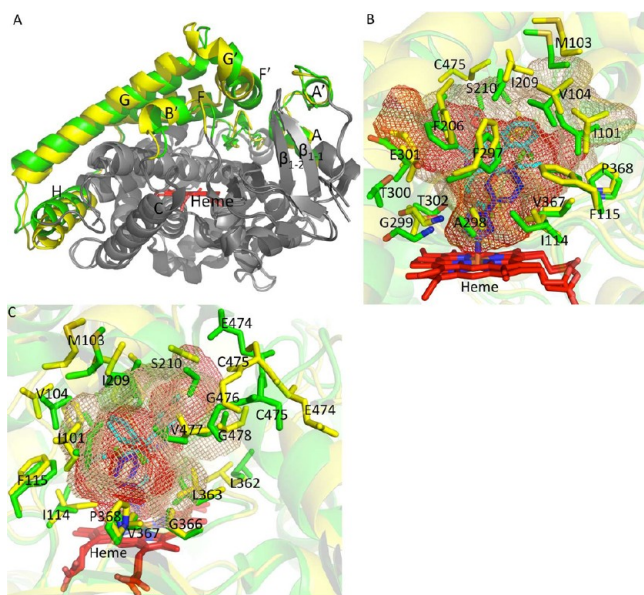


Figure 6. Overlay of human P450 2B6 structures. (A) P450 2B6 complexed with amlodipine and 4CPI (PDB entry 3IBD) superimposed onto each other with differences in secondary structural elements colored yellow and green, respectively. Amlodipine and 4CPI were deleted for the sake of clarity. (B and C) Overlay of cavity volume and residues in sticks lining the active sites of P450 2B6–amlodipine (yellow) and P450 2B6–4CPI (green) complexes (these panels are orthogonal views of the same figure). The cavity volume of the amlodipine complex and the 4CPI complex of P450 2B6 are shown as brown and red mesh, respectively.

to the C-terminal end close to the β_{3-2} sheet in the amlodipine complexes of P450 2B4 and P450 2B6.

As shown in panels B and C of Figure 6, the active site of the P450 2B6–amlodipine complex extends to residues F115, S210, G299, T300, E301, L362, G366, P368, and G478, which were not found to be a part of the P450 2B6–4CPI binding pocket. The calculated volume of the P450 2B6 active site cavity is 755 Å³ compared with the previously observed volume for the P450 2B6–4CPI complex of 582 Å³.⁸ Residues I101, M103, and V104 on helix B' and I209 and S210 on helix F in the P450 2B6–amlodipine complex structure are now shifted out even more compared with those in the 4CPI complex or the P450 2B4–amlodipine complex, and this contributes to the significant increase in the cavity dimensions compared with those of the other structures. Additionally, movement of residues 474–477 with the C α atom of E474 and C475 displaced by as much as ~3 Å expands the volume of the cavity to accommodate amlodipine within the active site. Differences in the cavity volume between the two P450 2B6 complexes also reflect the movement of phenylalanine side chains as observed with P450 2B4.

Interestingly, the part of the cavity bounded by residues T300, E301, and T302 on helix I is actually reduced in volume in the amlodipine structure compared with the 4CPI complex. Specifically, the side chain of E301 now protrudes into the cavity observed in the 4CPI complex. Moreover, as observed previously in the 4BP complex,¹⁵ the side chain of L362 swings in by 90° toward the active site and directs T302 into the proximity of the amlodipine molecule.

Differences in Specific Amlodipine Interactions between P450 2B4 and P450 2B6. An overlay of the P450 2B4– and P450 2B6–amlodipine structures (Figure 6 of

the Supporting Information) resulted in an rmsd of 0.66 Å and revealed considerable differences in the C–D loop, H–I loop, C-terminal loop, and β_{1-1} and β_{1-2} sheets, which bulge out more toward the solvent in the P450 2B4 structure (inset of Figure 6 of the Supporting Information). The only polar residue interaction evident between the proteins and amlodipine within the hydrophobic active site is that with T302. This side chain in the P450 2B4–amlodipine complex makes a hydrogen bond with the pyridine nitrogen of amlodipine, while the polar side chain of T302 interacts with the ethoxy oxygen of amlodipine within the active site of P450 2B6 (Figure 7A,B of the Supporting Information). Moreover, the distinct orientation of the second amlodipine in the two structures revealed interesting differences in polar interactions with this molecule. In P450 2B4, hydrogen bonding occurs between the primary amine of this amlodipine molecule, which extends into substrate access channel 2a, and the carboxylate of E387 on the β_{1-3} sheet (Figure 7A of the Supporting Information). Interestingly, the alternate conformation of this molecule located in substrate access channel 2f in the P450 2B6 structure now allows the polar side chain of Q215 to hydrogen bond with the pyridine nitrogen and ethoxy oxygen of the amlodipine (Figure 7B of the Supporting Information). However, Q215 and the pyridine nitrogen and ethoxy oxygen of amlodipine contact a water molecule in the P450 2B4 structure.

Ligand Docking. Computer-aided docking was used to explore the utility of the amlodipine-bound complexes of P450 2B4 and P450 2B6 in predicting protein–ligand interactions of larger drugs. First, the methodology was validated by docking amlodipine, which inhibited P450 2B4 and 2B6 with IC₅₀ values of 2 and 1.6 μM, respectively. Subsequently, two larger compounds, the selective estrogen receptor modulator raloxifene (MW = 473.5 g/mol) and the antifungal agent itraconazole (MW = 705.5 g/mol), were studied. Both have been shown previously to be among the most potent inhibitors of P450 2B6.²⁹ As presented in more detail below, amlodipine runs produced the largest variations in binding site, and raloxifene runs produced binding events predominantly in the active site or substrate access channel 2f. While itraconazole runs largely produced poses with the imidazole end of the molecule located in the active site, roughly equal numbers of poses placed the imidazole or the *p*-chloro of the dichlorophenyl group closest to the heme iron. Representative poses of P450 2B6 docking experiments are shown in Figure 7.

Amlodipine. As expected, this molecule adopted multiple poses in the active site and substrate access channels of both P450 2B4 and P450 2B6; the energy distributions were roughly equal for rigid poses (−7.4 to −5.4 kcal mol^{−1} for P450 2B4 and −7.5 to −5.2 kcal mol^{−1} for P450 2B6). Docking utilizing P450 2B4 as a receptor produced a variety of poses of a single molecule of amlodipine. These were distributed (1) throughout the active site, (2) partially in the solvent access channel, (3) in substrate access channels 2a and 2f as in the structure, (4) only in substrate access channel 2f, or (5) in various locations across the enzyme's external surface. With P450 2B6 as the receptor, most poses were (1) in the active site, (2) solely in channel 2f, or (3) at the interface of substrate access channels 2a and 2f. The three-lowest affinity poses were located between the C- and H-helices on the periphery of the enzyme. In each experiment, the most populated poses that include the one with the highest affinity for P450 2B4 and P450 2B6 had the

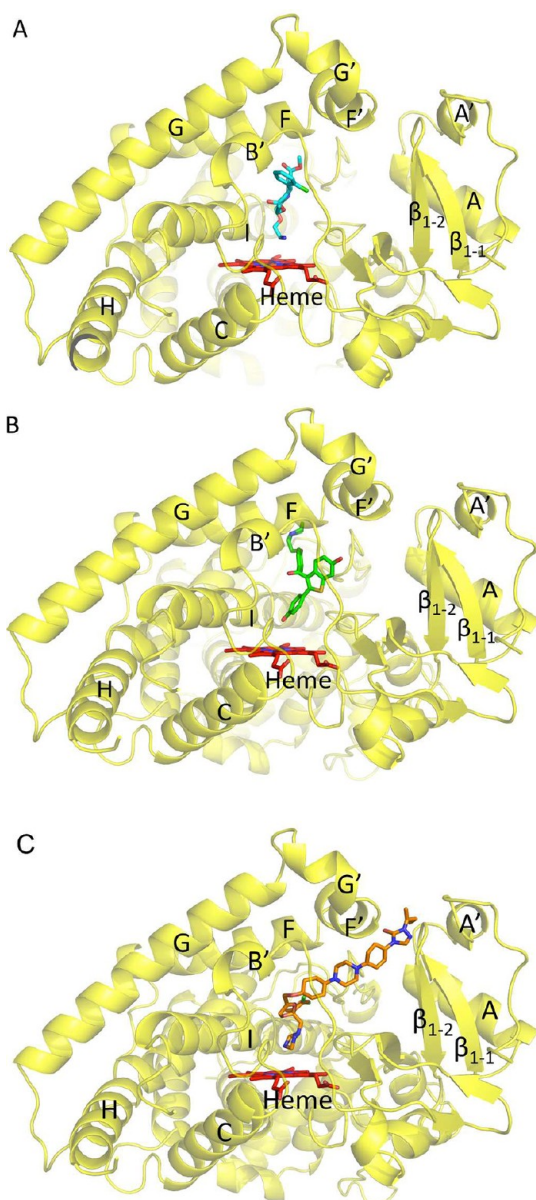


Figure 7. Representative pose showing amlodipine (cyan sticks), raloxifene (green sticks), and itraconazole (orange sticks) docking using the P450 2B6–amlodipine structure shown as a yellow ribbon. Heme is shown as red sticks. (A) Docking of amlodipine shows the amine nitrogen oriented toward the heme iron in the highest-affinity pose consistent with the X-ray crystal structure. (B) Raloxifene docking with the hydroxyphenyl oriented toward the heme as the lowest-energy and highest affinity pose located within the active site in P450 2B6. (C) Depiction of itraconazole with the imidazole nitrogen facing the heme in the most populous and highest-affinity poses.

terminal amine nitrogen oriented toward the heme iron in the active site (Figure 7A).

Raloxifene. For both P450 2B4 and P450 2B6, all poses were found in the active site, substrate access channel 2f, or at the interface of these two regions; docked complexes resulted in similar energy distributions for the two enzymes in the rigid docking events (-10.1 to -9.4 kcal mol $^{-1}$ for P450 2B4 and -10.8 to -9.5 kcal mol $^{-1}$ for P450 2B6). For P450 2B4, raloxifene showed approximately equal preference for the active site or the substrate access channel interface involving mainly channel 2f. In contrast, raloxifene was found in the active site of

P450 2B6 in the 18 events with the lowest energy, the junction of substrate access channels 2a and 2f in one event, and at the interface of the active site and the substrate access channels in one event. The majority of the clusters within the active site had either the hydroxyphenyl group or the thiophene group closer to the heme. Moreover, the thiophene group was facing the heme iron in the highest-affinity pose with P450 2B4, whereas P450 2B6 had the hydroxyphenyl group toward heme in the highest-affinity orientation (Figure 7B).

Itraconazole. This relatively linear molecule adopted multiple poses in the active sites and access channels of both P450 2B4 and P450 2B6, and the energy distributions were comparable for both enzymes (-10.9 to -8.5 kcal mol $^{-1}$ for P450 2B4 and -11.5 to -8.5 kcal mol $^{-1}$ for P450 2B6). Events with P450 2B4 as the receptor produced 17 poses with part of the ligand in the active site and the remainder protruding into substrate access channel 2f or exiting the solvent access channel; three poses bridged substrate access channels 2a and 2f and did not enter the active site. Similarly, P450 2B6 produced 17 poses, 16 of which entered the active site and one of the access channels, while one pose was on the distal face of the protein. With each of the proteins mentioned above, the highest-affinity pose of itraconazole in the active site had the imidazole nitrogen facing the heme iron as shown in Figure 7C.

Spectral Binding Titrations. To confirm the orientation of the first amlodipine molecule, spectral binding titrations were performed with both P450 2B4 and P450 2B6. As shown in Figure 8 of the Supporting Information, amlodipine induced a type II spectrum in P450 2B4 indicative of an iron–nitrogen coordinate bond. The spectral dissociation constant (K_s) from three independent experiments was 2.06 ± 0.37 μ M for P450 2B4, which is very similar to the IC_{50} . The maximal percent conversion to the type II complex was $23 \pm 3\%$. P450 2B6 produced a type II spectral change and a binding affinity upon addition of amlodipine similar to those of P450 2B4 (data not shown).

DISCUSSION

The first structure of human P450 2B6 in complex with a drug and the P450 2B4 complex determined by X-ray crystallography in this study show the existence of substrate access channels in these enzymes. The detailed information obtained advances significantly our mechanistic understanding of how P450s recognize and bind larger drugs and the conformational changes that a P450 undergoes in the process. Previous *in silico* studies of several mammalian and bacterial P450s, including P450 2C9, P450 3A4, P450 101A1, and P450 2A6,^{23,51,60,61} have used MD simulations to predict the presence of a substrate entrance pathway that connects the active site and the surface of the protein. Channels 2f and 2a in P450 2C9 have been suggested on the basis of MD simulations to point toward substrate access, whereas the solvent channel is hypothesized to be involved in metabolite egress. However, substrate access channel 2f was found mostly closed in the simulations performed for P450 2C9 and was thought to facilitate wider opening of the protein by merging with channel 2a.⁵¹ A similar MD study using the P450 2C9 substrate ibuprofen also suggested that channels 2f and 2a could be important for substrate binding, whereas the solvent channel is involved in metabolite release.⁵² Our X-ray structures indicate that both amlodipine molecules could have entered the active site via channel 2f in human P450 2B6 and rabbit P450 2B4 as well as

via the additional channel 2a in P450 2B4. However, the possibility remains that the first amlodipine molecule enters the protein via several available channels, with the more distal amlodipine molecule representing a secondary binding site after the binding of first amlodipine to the heme. The precise role of the solvent channel lined with several hydrophilic residues remains unknown; nevertheless, it is accessible for ligands to enter or exit from protein exterior. Furthermore, results from computer-aided docking corroborated structural studies and the use of these channels for substrate access to fit not only amlodipine into the active site pocket but also other 2B ligands as large as raloxifene and itraconazole.

Multiple binding of ligands has been observed previously with P450 3A4–ketoconazole and P450 2C8–9-*cis*-retinoic acid complexes, but the second ligand molecule was confined to the active site and packed on top of the first molecule near the heme.^{17,62} Recent structural analysis of P450 2A13 found two NNK molecules in a closed conformation of the protein.²⁴ From a structural overlay with the current 2B4–amlodipine complex (Figure 9 of the Supporting Information), it appears that the second NNK molecule in P450 2A13 is located right at the interface of the solvent channel and channel 2a. However, neither channel 2a nor channel 2f was observed in the dual ligand complex of P450 2A13 as a result of the closing of helices F, F', G', and G and the β_4 sheet system, which retracted as much as 4 Å compared to the current 2B structures bound to amlodipine. Clearly, the presence of a solvent channel, which was also observed in the recent P450 2D6 structure,⁵⁷ suggests a possible route for the entry of ligand into these enzymes that is located near the β_4 sheets and helix F. Interestingly, the second molecule of 17 α -hydroxyprogesterone in the P450 21A2²⁵ complex is in a perfect overlay with the second molecule of amlodipine in channel 2a of P450 2B4, further illustrating the use of different substrate access routes in various cytochrome P450s.

Interestingly, a CYMAL-5 molecule has been shown to be located at the interface of channel 2f and the surface of the protein in several P450 2B4 and P450 2B6 structures determined previously (Figure 10 of the Supporting Information).^{14,15,63} In addition, the P450 2B4–ticlopidine complex shows a different detergent molecule (232-chol) located at the 2f channel entrance close to helix F' where CYMAL-5 has been observed. This is indicative of a putative surface recognition site in P450 2B4 and P450 2B6 prior to the entry of ligand into the protein. Positioning P450 2B4 and P450 2B6 as described previously with P450 2C9⁵² shows that channels 2a and 2f are located within the membrane (Figure 8), and the solvent channel is close to the membrane–water interface. The residues that interact with CPR in the cytosol are also shown. This representation mimics the mechanism previously proposed,^{23,51} where the substrate molecule, amlodipine in this case, enters access channel 2f (or 2a for P450 2B4), and the polar metabolite is then released into the cytosol via the solvent channel. Moreover, membrane insertion predictions for P450s 2B4 and 2B6 were made using the Orientations of Proteins in Membranes server.⁶⁴ The location of channel 2f pointing toward the membrane further suggests that this is the major route for the access of the substrate to P450 2B4 and P450 2B6. Furthermore, a CYMAL-5 molecule could also be seen pointing from the membrane into channel 2f upon similar analysis of the 2B4–ticlopidine complex.

In addition to P450 2C9, channel 2a has been suggested via MD simulation to be one of the channels used for substrate

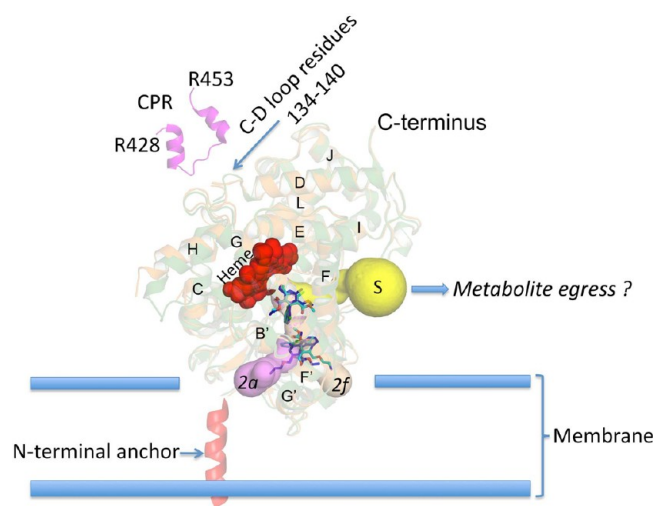


Figure 8. Cartoon of substrate access and solvent channels in P450 2B4 and P450 2B6 based on the current study with the enzymes anchored to the membrane via N-terminal residues (adopted from ref 52). Amlodipine molecules (blue and cyan) are shown to enter the protein via substrate access channel 2a or 2f of rabbit P450 2B4 and channel 2f of human P450 2B6. The possible exit route for metabolites via the solvent channel (S) is also shown. Residues of CPR (428–453, magenta) shown previously⁴² to bind in the C–D loop region (residues 134–140) are located at the proximal side of the protein predicted to lie within the cytosol.

access in P450 3A4⁵⁶ and proposed as the main ligand exit channel in some bacterial P450s.⁶⁰ The opening of channel 2a in the P450 2B4–amlodipine complex is caused by the shift of the R73 side chain. In a protein alignment, R73 of P450 2B4 aligns to K72 of P450 2C9 and R47 of P450 BM3, both of which are proposed to interact with the substrate and play an important role in recognition at the substrate access channel entrance.^{65,66} The side chain of K72 in P450 2C9 makes a similar turn at the β_{1-1} and β_{1-2} sheets,⁶⁷ closing channel 2a, similar to what is observed in P450 2B6 or the closed conformations of P450 2B4. In addition, recent structural analysis of rat mitochondrial P450 24A1 in the presence of multiple detergent molecules showed that membrane-directed substrate access channel 2a is the major access route.²⁷ Interestingly, F104 in P450 24A1, which was predicted to be one of the important residues to line the membrane-accessible substrate access channel described above, aligns with R73 in P450 2B4.

The availability of the new P450 2B4–amlodipine complex allows us to extract considerably more detail from two previously determined structures containing two or more molecules of imidazole inhibitors.^{11,12} An overlay of the structures of the amlodipine and bifonazole complexes revealed that the position of a second bifonazole molecule coincides with the entrance of the 2f channel observed in the current structure (Figure 11 of the Supporting Information). This structural evidence is supported by a recent computational analysis that suggested that channel 2f is used for bifonazole access in P450 2B4.⁶⁸ Moreover, superimposing the P450 2B4–amlodipine complex and the triple-ligand occupancy structure of P450 2B4 with 1-biphenyl-4-methyl-1H-imidazole (1PBI)¹² positions one molecule of 1PBI at the entrance of channel 2a (Figure 12 of the Supporting Information). Interestingly, the side chain of R73 bulges out toward the solvent in the 1PBI complex, further supporting our hypothesis

of a putative substrate recognition residue involved in channel opening. In addition, the open ligand-free structure of P450 2B4 demonstrated a wide opening of channel 2a to allow another protein molecule into the active site.⁶⁹ Thus, although the markedly open conformations observed due to dimerization of these previous P450 2B4 structures precluded the precise determination of substrate access channels, the results are very consistent with the channels that are now apparent from the P450 2B4–amlodipine complex.

Recent analysis of P450_{cam} structures¹⁶ revealed several conformational states that contained significant differences in the locations of helices B', F, and G and the F–G loop and to some extent helices C, H, and I, which are close to the substrate access channel. Furthermore, the amlodipine complexes of P450 2B4 and P450 2B6 display conformational changes largely similar to those in P450_{cam}. This is in sharp contrast to earlier studies using imidazoles or ligand-free P450 2B4, which showed much more wide-open conformations. In that context, it is noteworthy that recent MD simulations of several P450s indicate substrate-induced conformational changes that allow substrate access without a large opening of the protein.⁷⁰

Analysis of adaptive changes within the hydrophobic active sites of P450 2B4 and P450 2B6 reveals the polar interaction of T302 with the inner amlodipine and distinct polar interactions of E387 and Q215 with the outer amlodipine in P450 2B4 and P450 2B6, respectively. In addition, residue E218 on helix F' located at the intersection of substrate access channels 2a and 2f in P450 2B4 is retracted substantially in both enzymes, now allowing amlodipine access (Figure 13 of the Supporting Information). Gating of this entrance by movement of E218 allows hydrogen bonding between E387 or Q215 and amlodipine. Moreover, E218 aligns structurally with E222 in P450 2D6, which has been proposed recently as the “bait” for guiding initial substrate binding or entry and proper orientation for metabolism.⁵⁷ Interestingly, the E222A mutant in P450 2D6 has exhibited significantly altered ligand binding,⁷¹ and the corresponding polar residue in P450 3A4 and P450 2C9 is critical for the productive orientation of the ligand.^{72,73}

In conclusion, the crystal structures of drug-metabolizing enzymes presented here reveal two amlodipine molecules bound and show several possible substrate access channels in human P450 2B6 and rabbit P450 2B4. These structures also provide valuable insight into how active site topology is altered to accommodate large and/or multiple drug molecules. In addition to residues E218 and E387 or Q215 described above, the residues located at the respective substrate access channel entrance in human P450 2B6 and rabbit P450 2B4 could be crucial in substrate recognition, and efforts are underway to explore the functional role of these residues. Finally, these new structures of P450 2B6 and 2B4 in a conformation with an enlarged active site are amenable to the docking of larger drug molecules as demonstrated here and will serve as important in silico models for the design of novel drugs. Additional crystal structures of these enzymes with non-nitrogenous ligands will help explain how enzymes from different species recognize and bind the same drug.

■ ASSOCIATED CONTENT

● Supporting Information

Table showing the active site residues located within 5 Å of amlodipine molecules in P450 2B4 and P450 2B6, a diagram showing the amlodipine structure, a figure showing an orthogonal stereoview of amlodipine electron density in P450

2B4 and P450 2B6 complexes, figures showing the residues lining the solvent channel in P450 2B4 and P450 2B6 and an overlay with the corresponding 4-CPI complexes, an overlay of P450 2B6 and P450 2B4 structures showing differences near the C-terminal region, an overlay of P450 2B4– and P450 2B6–amlodipine complexes, structures of P450 2B4 and P450 2B6 showing interactions with amlodipine, a difference spectrum of P450 2B4 representative of a type II change upon amlodipine binding, an overlay of the P450 2B4–amlodipine complex with the P450 2A13–NNK structure, an overlay of various P450 2B4 and P450 2B6 complexes showing the location of the CYMAL-5 molecule at the 2f substrate access channel entrance, figures showing an overlay of the P450 2B4–amlodipine complex with the P450 2B4–bifonazole and P450–1PBI complexes, and an overlay of P450 2B4– and P450 2B6–amlodipine and 4-CPI complexes showing the location of residue E218. This material is available free of charge via the Internet at <http://pubs.acs.org>.

■ Accession Codes

Atomic coordinates and structure factors for the P450 2B4–amlodipine and 2B6–amlodipine complexes are deposited in the Protein Data Bank as entries 3TMZ and 3UA5, respectively.

■ AUTHOR INFORMATION

Corresponding Author

*E-mail: m7shah@ucsd.edu. Telephone: (858) 822-7804. Fax: (858) 246-0089.

Funding

This research was supported by National Institutes of Health Grants ES003619 to J.R.H. and GM098538 to Q.Z.

Notes

The authors declare no competing financial interest.

■ ACKNOWLEDGMENTS

We are grateful to Dr. Sean Gay for critical reading of the manuscript. We thank Dr. Dmitri Davydov for assistance with SpectraLab software and Dr. Deepak Dalvie for helpful discussions. We also thank the staff at the Stanford Synchrotron Radiation Lightsource, operated by Stanford University on behalf of the U.S. Department of Energy, Office of Basic Energy Sciences, for assistance with data collection. The Stanford Synchrotron Radiation Lightsource is supported by the National Institutes of Health, the National Center for Research Resources, the Biomedical Technology Program, and the U.S. Department of Energy of Biological and Environmental Research.

■ ABBREVIATIONS

P450, cytochrome P450; DTT, dithiothreitol; BME, 2-mercaptoethanol; PMSE, phenylmethanesulfonyl fluoride; CYMAL-5, 5-cyclohexyl-1-pentyl- β -D-maltoside; EDTA, ethylenediaminetetraacetic acid; 4CPI, 4-(4-chlorophenyl)imidazole; 1PBI, 1-biphenyl-4-methyl-1H-imidazole; Ni²⁺-NTA, nickel-nitrilotriacetic acid; 232-chol, 3 α ,7 α ,12 α -tris[(β -D-maltopyranosyl)ethoxy]cholane; SSRL, Stanford Synchrotron Radiation Lightsource; BL, beamline; rmsd, root-mean-square deviation; PDB, Protein Data Bank; 234-chol, 3(R)-hydroxy-7(R),12(R)-bis[([2(trimethylamino)ethyl]phosphoryl)-ethoxy]cholane; MD, molecular dynamics; 7-EFC, 7-ethoxy-4-(trifluoromethyl)coumarin; 7-MFC, 7-methoxy-4-(trifluoromethyl)coumarin; CPR, cytochrome P450 reductase;

4BP, 4-benzylpyridine; 4NBP, 4-(4-nitrobenzyl)pyridine; NADPH, reduced nicotinic adenine dinucleotide phosphate; CHAPS, 3-[(3-cholamidopropyl)dimethylammonio]-1-propanesulfonate; DMSO, dimethyl sulfoxide.

■ ADDITIONAL NOTES

^aThe initial P450 2B4 X-ray crystal structure was determined using a truncated and modified protein containing the wild-type His226. Because of the formation of a dimer involving coordination of His226 of each monomer with the heme iron of the other monomer, subsequent biochemical and crystallography work utilized the H226Y mutant. In this work, P450 2B4 will refer to P450 2B4dH(H226Y) unless otherwise stated.

^bP450 2B6 stands for an N-terminally truncated and modified and C-terminally His-tagged form of the cytochrome P450 2B6 genetic variant K262R with an internal Y226H mutation.

■ REFERENCES

- (1) Ortiz de Montellano, P. R. (2005) *Cytochrome P450: Structure, Mechanism and Biochemistry*, 3rd ed., Kluwer Academic/Plenum Publishers, New York.
- (2) Johnson, E. F., and Stout, C. D. (2005) Structural diversity of human xenobiotic-metabolizing cytochrome P450 monooxygenases. *Biochem. Biophys. Res. Commun.* 338, 331–336.
- (3) Black, S. D., Martin, S. T., and Smith, C. A. (1994) Membrane topology of liver microsomal cytochrome P450 2B4 determined via monoclonal antibodies directed to the halt-transfer signal. *Biochemistry* 33, 6945–6951.
- (4) Scott, E. E., Spatzenegger, M., and Halpert, J. R. (2001) A truncation of 2B subfamily cytochromes P450 yields increased expression levels, increased solubility, and decreased aggregation while retaining function. *Arch. Biochem. Biophys.* 395, 57–68.
- (5) Scott, E. E., Liu, H., Qun, H. Y., Li, W., and Halpert, J. R. (2004) Mutagenesis and molecular dynamics suggest structural and functional roles for residues in the N-terminal portion of the cytochrome P450 2B1 I helix. *Arch. Biochem. Biophys.* 423, 266–276.
- (6) Zhao, Y., and Halpert, J. R. (2007) Structure-function analysis of cytochromes P450 2B. *Biochim. Biophys. Acta* 1770, 402–412.
- (7) Wilderman, P. R., Shah, M. B., Liu, T., Li, S., Hsu, S., Roberts, A. G., Goodlett, D. R., Zhang, Q., Woods, V. L., Jr., Stout, C. D., and Halpert, J. R. (2010) Plasticity of cytochrome P450 2B4 as investigated by hydrogen-deuterium exchange mass spectrometry and X-ray crystallography. *J. Biol. Chem.* 285, 38602–38611.
- (8) Gay, S. C., Roberts, A. G., and Halpert, J. R. (2010) Structural features of cytochromes P450 and ligands that affect drug metabolism as revealed by X-ray crystallography and NMR. *Future Med. Chem.* 2, 1451–1468.
- (9) Gay, S. C., Zhang, H., Wilderman, P. R., Roberts, A. G., Liu, T., Li, S., Lin, H. L., Zhang, Q., Woods, V. L., Jr., Stout, C. D., Hollenberg, P. F., and Halpert, J. R. (2011) Structural analysis of mammalian cytochrome P450 2B4 covalently bound to the mechanism-based inactivator tert-butylphenylacetylene: Insight into partial enzymatic activity. *Biochemistry* 50, 4903–4911.
- (10) Scott, E. E., He, Y. A., Wester, M. R., White, M. A., Chin, C. C., Halpert, J. R., Johnson, E. F., and Stout, C. D. (2003) An open conformation of mammalian cytochrome P450 2B4 at 1.6-Å resolution. *Proc. Natl. Acad. Sci. U.S.A.* 100, 13196–13201.
- (11) Zhao, Y., White, M. A., Muralidhara, B. K., Sun, L., Halpert, J. R., and Stout, C. D. (2006) Structure of microsomal cytochrome P450 2B4 complexed with the antifungal drug bifonazole: Insight into P450 conformational plasticity and membrane interaction. *J. Biol. Chem.* 281, 5973–5981.
- (12) Gay, S. C., Sun, L., Maekawa, K., Halpert, J. R., and Stout, C. D. (2009) Crystal structures of cytochrome P450 2B4 in complex with the inhibitor 1-biphenyl-4-methyl-1H-imidazole: Ligand-induced structural response through α -helical repositioning. *Biochemistry* 48, 4762–4771.
- (13) Zanger, U. M., Klein, K., Saussele, T., Bliedernicht, J., Hofmann, M. H., and Schwab, M. (2007) Polymorphic CYP2B6: Molecular mechanisms and emerging clinical significance. *Pharmacogenomics* 8, 743–759.
- (14) Gay, S. C., Shah, M. B., Talakad, J. C., Maekawa, K., Roberts, A. G., Wilderman, P. R., Sun, L., Yang, J. Y., Huelga, S. C., Hong, W. X., Zhang, Q., Stout, C. D., and Halpert, J. R. (2010) Crystal structure of a cytochrome P450 2B6 genetic variant in complex with the inhibitor 4-(4-chlorophenyl)imidazole at 2.0-Å resolution. *Mol. Pharmacol.* 77, 529–538.
- (15) Shah, M. B., Pascual, J., Zhang, Q., Stout, C. D., and Halpert, J. R. (2011) Structures of cytochrome P450 2B6 bound to 4-benzylpyridine and 4-(4-nitrobenzyl)pyridine: Insight into inhibitor binding and rearrangement of active site side chains. *Mol. Pharmacol.* 80, 1047–1055.
- (16) Lee, Y. T., Glazer, E. C., Wilson, R. F., Stout, C. D., and Goodin, D. B. (2011) Three clusters of conformational states in p450cam reveal a multistep pathway for closing of the substrate access channel. *Biochemistry* 50, 693–703.
- (17) Schoch, G. A., Yano, J. K., Sansen, S., Dansette, P. M., Stout, C. D., and Johnson, E. F. (2008) Determinants of cytochrome P450 2C8 substrate binding: structures of complexes with montelukast, troglitazone, felodipine, and 9-cis-retinoic acid. *J. Biol. Chem.* 283, 17227–17237.
- (18) Porubsky, P. R., Meneely, K. M., and Scott, E. E. (2008) Structures of human cytochrome P-450 2E1. Insights into the binding of inhibitors and both small molecular weight and fatty acid substrates. *J. Biol. Chem.* 283, 33698–33707.
- (19) Strushkevich, N., Usanov, S. A., Plotnikov, A. N., Jones, G., and Park, H. W. (2008) Structural analysis of CYP2R1 in complex with vitamin D3. *J. Mol. Biol.* 380, 95–106.
- (20) Mast, N., Charvet, C., Pikuleva, I. A., and Stout, C. D. (2010) Structural basis of drug binding to CYP46A1, an enzyme that controls cholesterol turnover in the brain. *J. Biol. Chem.* 285, 31783–31795.
- (21) Strushkevich, N., Usanov, S. A., and Park, H. W. (2010) Structural basis of human CYP51 inhibition by antifungal azoles. *J. Mol. Biol.* 397, 1067–1078.
- (22) Cojocaru, V., Balali-Mood, K., Sansom, M. S., and Wade, R. C. (2011) Structure and dynamics of the membrane-bound cytochrome P450 2C9. *PLoS Comput. Biol.* 7, e1002152.
- (23) Fishelovitch, D., Shaik, S., Wolfson, H. J., and Nussinov, R. (2009) Theoretical characterization of substrate access/exit channels in the human cytochrome P450 3A4 enzyme: Involvement of phenylalanine residues in the gating mechanism. *J. Phys. Chem. B* 113, 13018–13025.
- (24) Devore, N. M., and Scott, E. E. (2012) Nicotine and 4-(methylnitrosamino)-1-(3-pyridyl)-1-butanone (NNK) binding and access channel in human cytochrome P450 2A6 and 2A13 enzymes. *J. Biol. Chem.* 287, 26576–26585.
- (25) Zhao, B., Lei, L., Kagawa, N., Sundaramoorthy, M., Banerjee, S., Nagy, L. D., Guengerich, F. P., and Waterman, M. R. (2012) Three-dimensional structure of steroid 21-hydroxylase (cytochrome P450 21A2) with two substrates reveals locations of disease-associated variants. *J. Biol. Chem.* 287, 10613–10622.
- (26) Yang, W., Bell, S. G., Wang, H., Zhou, W., Bartlam, M., Wong, L. L., and Rao, Z. (2011) The structure of CYP101D2 unveils a potential path for substrate entry into the active site. *Biochem. J.* 433, 85–93.
- (27) Annalora, A. J., Goodin, D. B., Hong, W. X., Zhang, Q., Johnson, E. F., and Stout, C. D. (2010) Crystal structure of CYP24A1, a mitochondrial cytochrome P450 involved in vitamin D metabolism. *J. Mol. Biol.* 396, 441–451.
- (28) Murdoch, D., and Heel, R. C. (1991) Amlodipine. A review of its pharmacodynamic and pharmacokinetic properties, and therapeutic use in cardiovascular disease. *Drugs* 41, 478–505.
- (29) Walsky, R. L., Astuccio, A. V., and Obach, R. S. (2006) Evaluation of 227 drugs for in vitro inhibition of cytochrome P450 2B6. *J. Clin. Pharmacol.* 46, 1426–1438.

- (30) Zhang, Q., Ma, X., Ward, A., Hong, W. X., Jaakola, V. P., Stevens, R. C., Finn, M. G., and Chang, G. (2007) Designing facial amphiphiles for the stabilization of integral membrane proteins. *Angew. Chem., Int. Ed.* 46, 7023–7025.
- (31) DeLano, W. L. (2002) *The PyMOL Molecular Graphics System*, DeLano Scientific, Palo Alto, CA.
- (32) Omura, T., and Sato, R. (1964) The Carbon Monoxide-Binding Pigment of Liver Microsomes. I. Evidence for Its Hemoprotein Nature. *J. Biol. Chem.* 239, 2370–2378.
- (33) Mitsuda, M., and Iwasaki, M. (2006) Improvement in the expression of CYP2B6 by co-expression with molecular chaperones GroES/EL in *Escherichia coli*. *Protein Expression Purif.* 46, 401–405.
- (34) Soltis, S. M., Cohen, A. E., Deacon, A., Eriksson, T., Gonzalez, A., McPhillips, S., Chui, H., Dunten, P., Hollenbeck, M., Mathews, I., Miller, M., Moorhead, P., Phizackerley, R. P., Smith, C., Song, J., van dem Bedem, H., Ellis, P., Kuhn, P., McPhillips, T., Sauter, N., Sharp, K., Tsyba, I., and Wolf, G. (2008) New Paradigm for Macromolecular Crystallography Experiments at SSRL: Automated Crystal Screening and Remote Data Collection. *Acta Crystallogr. D* 64, 1210–1221.
- (35) Leslie, A. G. W. (1999) Integration of macromolecular diffraction data. *Acta Crystallogr. D* 55, 1696–1702.
- (36) Bailey, S. (1994) The CCP4 Suite: Programs for Protein Crystallography. *Acta Crystallogr. D* 50, 760–763.
- (37) McCoy, A. J., Grosse-Kunstleve, R. W., Adams, P. D., Winn, M. D., Storoni, L. C., and Read, R. J. (2007) Phaser crystallographic software. *J. Appl. Crystallogr.* 40, 658–674.
- (38) Murshudov, G. N., Vagin, A. A., and Dodson, E. J. (1997) Refinement of macromolecular structures by the maximum-likelihood method. *Acta Crystallogr. D* 53, 240–255.
- (39) Emsley, P., and Cowtan, K. (2004) Coot: Model-building tools for molecular graphics. *Acta Crystallogr. D* 60, 2126–2132.
- (40) Schüttelkopf, A. W., and van Aalten, D. M. (2004) PRODRG: A tool for high-throughput crystallography of protein-ligand complexes. *Acta Crystallogr. D* 60, 1355–1363.
- (41) Davis, I. W., Murray, L. W., Richardson, J. S., and Richardson, D. C. (2004) MOLPROBITY: Structure validation and all-atom contact analysis for nucleic acids and their complexes. *Nucleic Acids Res.* 32, W615–W619.
- (42) Bumpus, N. N., and Hollenberg, P. F. (2010) Cross-linking of human cytochrome P450 2B6 to NADPH-cytochrome P450 reductase: Identification of a potential site of interaction. *J. Inorg. Biochem.* 104, 485–488.
- (43) Long, F., Vagin, A. A., Young, P., and Murshudov, G. N. (2008) BALBES: A molecular-replacement pipeline. *Acta Crystallogr. D* 64, 125–132.
- (44) Petrek, M., Otyepka, M., Banas, P., Kosinova, P., Koca, J., and Damborsky, J. (2006) CAVER: A new tool to explore routes from protein clefts, pockets and cavities. *BMC Bioinf.* 7, 316.
- (45) Kleywegt, G. J., and Jones, T. A. (1994) Detection, delineation, measurement and display of cavities in macromolecular structures. *Acta Crystallogr. D* 50, 178–185.
- (46) Trott, O., and Olson, A. J. (2010) AutoDock Vina: Improving the speed and accuracy of docking with a new scoring function, efficient optimization, and multithreading. *J. Comput. Chem.* 31, 455–461.
- (47) Helms, V., and Wade, R. C. (1995) Thermodynamics of water mediating protein-ligand interactions in cytochrome P450cam: A molecular dynamics study. *Biophys. J.* 69, 810–824.
- (48) Harlow, G. R., and Halpert, J. R. (1997) Alanine-scanning mutagenesis of a putative substrate recognition site in human cytochrome P450 3A4. Role of residues 210 and 211 in flavonoid activation and substrate specificity. *J. Biol. Chem.* 272, 5396–5402.
- (49) Scott, E. E., White, M. A., He, Y. A., Johnson, E. F., Stout, C. D., and Halpert, J. R. (2004) Structure of mammalian cytochrome P450 2B4 complexed with 4-(4-chlorophenyl)imidazole at 1.9-Å resolution: Insight into the range of P450 conformations and the coordination of redox partner binding. *J. Biol. Chem.* 279, 27294–27301.
- (50) Zhang, H., Amunugama, H., Ney, S., Cooper, N., and Hollenberg, P. F. (2011) Mechanism-based inactivation of human cytochrome P450 2B6 by clopidogrel: Involvement of both covalent modification of cysteinyl residue 475 and loss of heme. *Mol. Pharmacol.* 80, 839–847.
- (51) Cojocaru, V., Balali-Mood, K., Sansom, M. S., and Wade, R. C. (2011) Structure and dynamics of the membrane-bound cytochrome P450 2C9. *PLoS Comput. Biol.* 7, e1002152.
- (52) Berka, K., Hendrychova, T., Anzenbacher, P., and Otyepka, M. (2011) Membrane Position of Ibuprofen Agrees with Suggested Access Path Entrance to Cytochrome P450 2C9 Active Site. *J. Phys. Chem. A* 115, 11248–11255.
- (53) Cojocaru, V., Winn, P. J., and Wade, R. C. (2007) The ins and outs of cytochrome P450s. *Biochim. Biophys. Acta* 1770, 390–401.
- (54) Rydberg, P., Rod, T. H., Olsen, L., and Ryde, U. (2007) Dynamics of water molecules in the active-site cavity of human cytochromes P450. *J. Phys. Chem. B* 111, 5445–5457.
- (55) Otyepka, M., Berka, K., and Anzenbacher, P. (2012) Is there a relationship between the substrate preferences and structural flexibility of cytochromes P450? *Curr. Drug Metab.* 13, 177–189.
- (56) Skopalik, J., Anzenbacher, P., and Otyepka, M. (2008) Flexibility of human cytochromes P450: Molecular dynamics reveals differences between CYPs 3A4, 2C9, and 2A6, which correlate with their substrate preferences. *J. Phys. Chem. B* 112, 8165–8173.
- (57) Wang, A., Savas, U., Hsu, M. H., Stout, C. D., and Johnson, E. F. (2012) Crystal structure of human cytochrome P450 2D6 with prinomastat bound. *J. Biol. Chem.* 287, 10834–10843.
- (58) Wilderman, P. R., Gay, S. C., Jang, H. H., Zhang, Q., Stout, C. D., and Halpert, J. R. (2012) Investigation by site-directed mutagenesis of the role of cytochrome P450 2B4 non-active-site residues in protein-ligand interactions based on crystal structures of the ligand-bound enzyme. *FEBS J.* 279, 1607–1620.
- (59) Wilderman, P. R., and Halpert, J. R. (2012) Plasticity of CYP2B Enzymes: Structural and Solution Biophysical Methods. *Curr. Drug Metab.* 13, 167–176.
- (60) Winn, P. J., Ludemann, S. K., Gauges, R., Lounnas, V., and Wade, R. C. (2002) Comparison of the dynamics of substrate access channels in three cytochrome P450s reveals different opening mechanisms and a novel functional role for a buried arginine. *Proc. Natl. Acad. Sci. U.S.A.* 99, 5361–5366.
- (61) Li, W., Shen, J., Liu, G., Tang, Y., and Hoshino, T. (2011) Exploring coumarin egress channels in human cytochrome P450 2A6 by random acceleration and steered molecular dynamics simulations. *Proteins* 79, 271–281.
- (62) Ekroos, M., and Sjogren, T. (2006) Structural basis for ligand promiscuity in cytochrome P450 3A4. *Proc. Natl. Acad. Sci. U.S.A.* 103, 13682–13687.
- (63) Gay, S. C., Roberts, A. G., Maekawa, K., Talakad, J. C., Hong, W. X., Zhang, Q., Stout, C. D., and Halpert, J. R. (2010) Structures of cytochrome P450 2B4 complexed with the antiplatelet drugs ticlopidine and clopidogrel. *Biochemistry* 49, 8709–8720.
- (64) Lomize, M. A., Lomize, A. L., Pogozheva, I. D., and Mosberg, H. I. (2006) OPM: Orientations of proteins in membranes database. *Bioinformatics* 22, 623–625.
- (65) Lewis, D. F., Dickens, M., Weaver, R. J., Eddershaw, P. J., Goldfarb, P. S., and Tarbit, M. H. (1998) Molecular modelling of human CYP2C subfamily enzymes CYP2C9 and CYP2C19: Rationalization of substrate specificity and site-directed mutagenesis experiments in the CYP2C subfamily. *Xenobiotica* 28, 235–268.
- (66) Haines, D. C., Tomchick, D. R., Machius, M., and Peterson, J. A. (2001) Pivotal role of water in the mechanism of P450BM-3. *Biochemistry* 40, 13456–13465.
- (67) Ravichandran, K. G., Boddupalli, S. S., Hasermann, C. A., Peterson, J. A., and Deisenhofer, J. (1993) Crystal structure of hemoprotein domain of P450BM-3, a prototype for microsomal P450's. *Science* 261, 731–736.
- (68) Otyepka, M., Berka, K., and Anzenbacher, P. (2012) Is there a relationship between the substrate preferences and structural flexibility of cytochromes P450? *Curr. Drug Metab.* 13, 130–142.

- (69) Wade, R. C., Winn, P. J., Schlichting, I., and Sudarko (2004) A survey of active site access channels in cytochromes P450. *J. Inorg. Biochem.* 98, 1175–1182.
- (70) Hendrychova, T., Berka, K., Navratilova, V., Anzenbacher, P., and Otyepka, M. (2012) Dynamics and hydration of the active sites of mammalian cytochromes P450 probed by molecular dynamics simulations. *Curr. Drug Metab.* 13, 177–189.
- (71) Masuda, K., Tamagake, K., Okuda, Y., Torigoe, F., Tsuzuki, D., Isobe, T., Hichiya, H., Hanioka, N., Yamamoto, S., and Narimatsu, S. (2005) Change in enantioselectivity in bufuralol 1''-hydroxylation by the substitution of phenylalanine-120 by alanine in cytochrome P450 2D6. *Chirality* 17, 37–43.
- (72) Sevrioukova, I. F., and Poulos, T. L. (2012) Structural and Mechanistic Insights into the Interaction of Cytochrome P4503A4 with Bromoergocryptine, a Type I Ligand. *J. Biol. Chem.* 287, 3510–3517.
- (73) Williams, P. A., Cosme, J., Ward, A., Angove, H. C., Matak Vinkovic, D., and Jhoti, H. (2003) Crystal structure of human cytochrome P450 2C9 with bound warfarin. *Nature* 424, 464–468.